scientific reports

Check for updates

OPEN

Vitamin D_3 suppresses Npt2c abundance and differentially modulates phosphate and calcium homeostasis in Npt2a knockout mice

Linto Thomas[1,2], Lashodya V. Dissanayake[1], Maryam Tahmasbi[3], Alexander Staruschenko[1,2,4], Sima Al-Masri[1], Jessica A. Dominguez Rieg[1,2,4] & Timo Rieg[1,2,4]✉

Vitamin D_3 is clinically used for the treatment of vitamin D_3 deficiency or osteoporosis, partially because of its role in regulating phosphate (P_i) and calcium (Ca^{2+}) homeostasis. The renal sodium-phosphate cotransporter 2a (Npt2a) plays an important role in P_i homeostasis; however, the role of vitamin D_3 in hypophosphatemia has never been investigated. We administered vehicle or vitamin D_3 to wild-type (WT) mice or hypophosphatemic Npt2a$^{-/-}$ mice. In contrast to WT mice, vitamin D_3 treatment increased plasma P_i levels in Npt2a$^{-/-}$ mice, despite similar levels of reduced parathyroid hormone and increased fibroblast growth factor 23. Plasma Ca^{2+} was increased ~ twofold in both genotypes. Whereas WT mice were able to increase urinary P_i and Ca^{2+}/creatinine ratios, in Npt2a$^{-/-}$ mice, P_i/creatinine was unchanged and Ca^{2+}/creatinine drastically decreased, coinciding with the highest kidney Ca^{2+} content, highest plasma creatinine, and greatest amount of nephrocalcinosis. In Npt2a$^{-/-}$ mice, vitamin D_3 treatment completely diminished Npt2c abundance, so that mice resembled Npt2a/c double knockout mice. Abundance of intestinal Npt2b and claudin-3 (tight junctions protein) were reduced in Npt2a$^{-/-}$ only, the latter might facilitate the increase in plasma P_i in Npt2a$^{-/-}$ mice. Npt2a might function as regulator between renal Ca^{2+} excretion and reabsorption in response to vitamin D_3.

Keywords Calcium, Fibroblast growth factor 23, Parathyroid hormone, Sodium-phosphate cotransporter, Vitamin D_3

Active vitamin D_3 or 1,25-dihydroxyvitamin D_3 ($1,25(OH)_2D_3$) is produced via the combined actions of skin, liver and kidneys[1]. Under normal conditions, it plays an essential role in the regulation of calcium (Ca^{2+}) and phosphate (P_i) homeostasis in the body[2]. A lack of vitamin D_3 can lead to rickets and other potential processes beyond bone health, including immune system dysregulation, development of cancer, or progression of cardiovascular disease[3]. The actions of vitamin D_3 are complex and involve hormones such as parathyroid hormone (PTH) and fibroblast growth factor 23 (FGF23)[4–6]. PTH and FGF23 are both phosphaturic hormones (via action on the renal Na^+-P_i transporters, Npt2a and Npt2c) which work collaboratively to maintain P_i homeostasis; however, this process involves a complicated regulatory role of $1,25(OH)_2D_3$[4,7]. $1,25(OH)_2D_3$ has opposing effects on these hormones: it enhances the production of FGF23 in bone, while simultaneously suppressing the synthesis of PTH[8,9]. In this complex feedback loop, where PTH and FGF23 normally promote renal P_i excretion, $1,25(OH)_2D_3$ may act as a switch between P_i excretion/absorption in order to maintain total body P_i[4]. The precursor of vitamin D_3, previtamin D_3, is formed by the skin and subsequently undergoes spontaneous isomerization to vitamin D_3, which has a half-life of ~ 26 h[10]. Any excess vitamin D_3 is stored mainly within fat tissue[11]. In the liver, an initial hydroxylation step takes place which converts vitamin D_3 into 25(OH) vitamin D_3.

[1]Department of Molecular Pharmacology and Physiology, Morsani College of Medicine, University of South Florida, Tampa, FL, USA. [2]James A. Haley Veterans' Hospital, Tampa, FL, USA. [3]Department of Pathology and Cell Biology, University of South Florida, Tampa, FL, USA. [4]Hypertension and Kidney Research Center, University of South Florida, Tampa, FL, USA. ✉email: trieg@usf.edu

After reaching the kidneys via the circulation, 25(OH) vitamin D_3 undergoes a second hydroxylation process to form $1,25(OH)_2D_3$[4,7]. PTH is part of a feedback loop that facilitates the production of $1,25(OH)_2D_3$ by inducing the transcription of renal 1α-hydroxylase, the enzyme responsible for this process[4]. Hormonal signaling of $1,25(OH)_2D_3$ is mediated by activation of the vitamin D receptor (VDR)[12] and many of its actions were described by studying VDR knockout ($VDR^{-/-}$) mice[13]. When $VDR^{-/-}$ mice mature on a control diet, they develop rickets because of hypophosphatemia, hypocalcemia, elevated plasma $1,25(OH)_2D_3$ and PTH levels[14]. This was found mainly to be the consequence of impaired intestinal P_i absorption rather than a renal P_i problem. Vice versa, administering $1,25(OH)_2D_3$ to wild-type mice (WT) led to enhanced intestinal P_i absorption[15], an effect absent in mice lacking the intestinal Na^+-P_i transporter (Npt2b)[15] implying a direct effect on transcellular P_i transport.

The importance of Npt2a for renal P_i reabsorption has been demonstrated in Npt2a knockout ($Npt2a^{-/-}$) mice. These mice are characterized by renal P_i wasting consequently leading to hypophosphatemia, hypoparathyroidism, reduced FGF23 levels and hypercalcemia[16–18]. Of note, effects of Npt2a knockout on plasma $1,25(OH)2D_3$ have shown to be increased[16,18] or unchanged[4]. This finding might be related to the age when mice are studied because $1,25(OH)2D_3$ levels decreased over time in $Npt2a^{-/-}$ mice between day 8 to day 35[19].

Despite these known factors, the effects of vitamin D_3 on P_i and Ca^{2+} regulation are incompletely understood, especially in the context of renal Npt2a and the involved complex regulatory pathways involving PTH and FGF23. In order to address this question, we treated mice lacking Npt2a ($Npt2a^{-/-}$) with vitamin D_3 and studied the impact on P_i and Ca^{2+} homeostasis. Our results demonstrate that vitamin D_3 plays a distinct role in regulating P_i homeostasis, Ca^{2+} balance, and suggest the existence of novel regulatory pathways involving functional Npt2a for the regulation of P_i homeostasis.

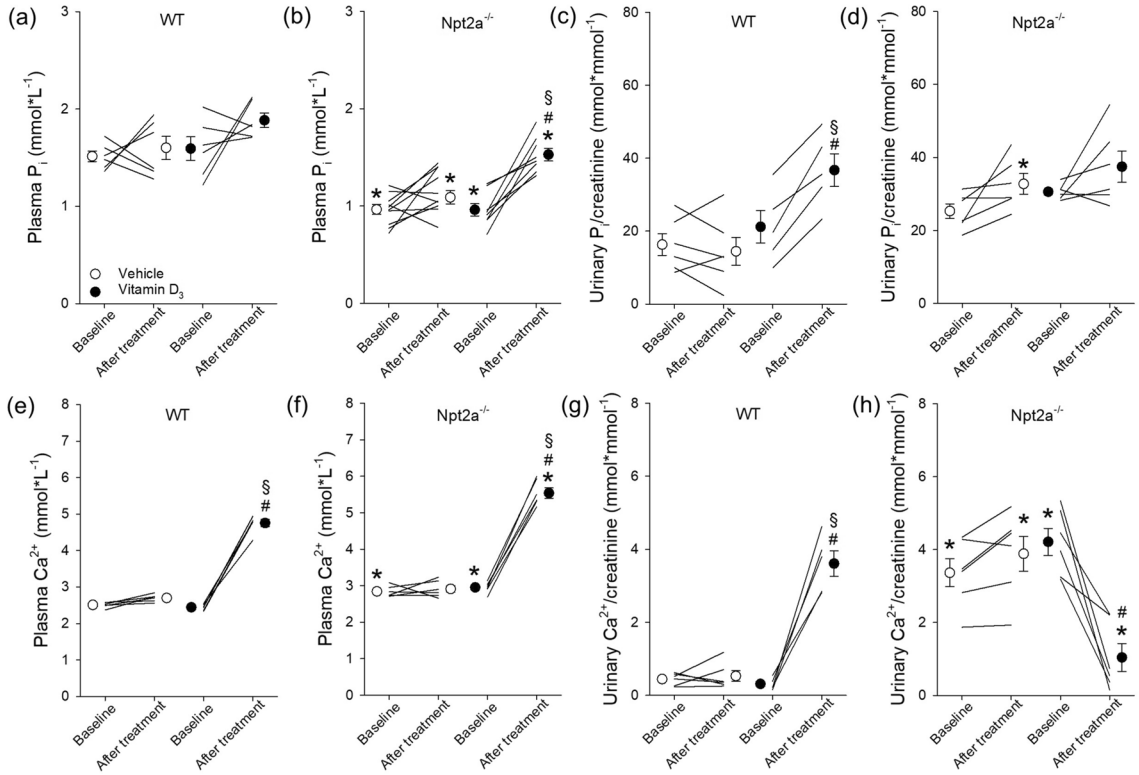

Figure 1. Lack of Npt2a unravels a link of vitamin D_3 on plasma P_i. Measurements of plasma and urinary P_i and Ca^{2+} were conducted in WT and $Npt2a^{-/-}$ mice after 4 days of treatment with either a vehicle or vitamin D_3 (n = 6–10 per genotype). (**a**) In WT mice, plasma P_i levels remained unchanged following vitamin D_3 treatment. (B) In contrast, lower plasma P_i levels under baseline conditions in $Npt2a^{-/-}$ mice significantly increased in response to vitamin D_3 treatment. (**c**) The urinary P_i/creatinine ratio in WT mice increased significantly in response to vitamin D_3 treatment. (**d**) This ratio in $Npt2a^{-/-}$ mice was unchanged (**d**). Plasma Ca^{2+} levels in both WT and $Npt2a^{-/-}$ mice showed a significant increase following vitamin D_3 treatment (**e** & **f**). In WT mice, the urinary Ca^{2+} to creatinine ratio significantly increased after vitamin D_3 treatment (**g**). In contrast, this ratio significantly decreased in $Npt2a^{-/-}$ mice (**h**). Male mice were used in these studies. In addition to single data summary data are shown and are expressed as mean ± SEM and were analyzed by repeated-measures two-way ANOVA followed by Tukey's multiple comparisons test. $^*P < 0.05$ vs WT same time point, $^{\#}P < 0.05$ vs baseline same genotype, $^{\S}P < 0.05$ vs vehicle same genotype and time point.

Results

Lower plasma P_i and a greater increase of plasma P_i in response to vitamin D_3 treatment in Npt2a$^{-/-}$ compared to WT mice

Consistent with previous reports[16,20], plasma P_i in Npt2a$^{-/-}$ mice was significantly lower compared to WT mice (Fig. 1a,b). In WT mice, neither vehicle treatment nor vitamin D_3 (300,000 IU/kg body weight) treatment affected plasma P_i levels (Fig. 1a). In contrast, plasma P_i significantly increased in Npt2a$^{-/-}$ mice (~ 1.6-fold), whereas vehicle treatment was without effect (Fig. 1b). Under baseline conditions, urinary P_i/creatinine ratios were not significantly different between genotypes (Fig. 1c,d). In WT mice, the urinary P_i/creatinine ratio remained unaltered in response to vehicle treatment but vitamin D_3 treatment resulted in a significant increase (~ 1.7-fold) compared to baseline (Fig. 1c). No significant changes were observed in urinary P_i/creatinine ratios in response to vehicle or vitamin D_3 treatment in Npt2a$^{-/-}$ mice (Fig. 1d).

Npt2a$^{-/-}$ mice showed significantly higher plasma Ca^{2+} levels (~ 1.2-fold) compared to WT mice (Fig. 1e,f). Vehicle treatment did not affect plasma Ca^{2+} levels (Fig. 1e,f) in WT or Npt2a$^{-/-}$ mice. Vitamin D_3 treatment significantly increased plasma Ca^{2+} in WT (~ 2.0-fold) and Npt2a$^{-/-}$ (~ 1.8-fold) mice. Of note, plasma Ca^{2+} was significantly greater in Npt2a$^{-/-}$ mice compared to WT mice in response to vitamin D_3 treatment (Fig. 1e,f). Under baseline conditions, urinary Ca^{2+}/creatinine ratios were significantly greater in Npt2a$^{-/-}$ compared to WT mice (Fig. 1g,h). In WT mice, the urinary Ca^{2+}/creatinine ratio remained unaltered in response to vehicle treatment; however, consistent with increased plasma Ca^{2+} in response to vitamin D_3 treatment, the urinary Ca^{2+}/creatinine ratio was appropriately increased (~ 11-fold). In contrast to WT mice, the urinary Ca^{2+}/creatinine ratio in Npt2a$^{-/-}$ mice was significantly decreased (~ 50%) in response to vitamin D_3 treatment; vehicle treatment was without effect (Fig. 1h).

Using a smaller dose of vitamin D_3 (3000 IU/kg body weight) showed no significant effects on plasma P_i or urinary P_i/creatinine ratios between genotypes (Supplementary Fig. 1a,b). Whereas plasma Ca^{2+} and urinary Ca^{2+}/creatinine ratios were not affected by vitamin D_3 in WT mice (Supplementary Fig. 1c,d), in Npt2a$^{-/-}$ mice, plasma Ca^{2+} and urinary Ca^{2+}/creatinine ratios significantly increased (~ 1.05-fold and ~ 2.7-fold, respectively).

Npt2a$^{-/-}$ mice lack PTH responses but FGF23 levels were significantly increased in response to vitamin D_3 treatment

Npt2a$^{-/-}$ mice show significantly lower plasma PTH levels under baseline conditions (Fig. 2a,b). In WT mice, plasma PTH showed a small but significant decrease in response to vehicle treatment (Fig. 2a). Vitamin D_3 treatment significantly decreased (~ 85%) plasma PTH (Fig. 2a) in WT mice. No significant changes in plasma PTH were observed in response to vehicle or vitamin D_3 treatment in Npt2a$^{-/-}$ mice (Fig. 2b). In addition to lower PTH levels in Npt2a$^{-/-}$ mice under baseline conditions, FGF23 levels were also significantly lower (~ 50%) compared to WT mice (Fig. 2c,d). Vehicle treatment did not significantly change FGF23 levels in either genotype (Fig. 2c,d). Vitamin D_3 treatment caused a significant increase of FGF23 levels in both genotypes: in WT mice an ~ 80-fold increase was observed, whereas in Npt2a$^{-/-}$ mice a ~ 200-fold increase was observed. The more than double increase of FGF23 in Npt2a$^{-/-}$ compared to WT mice in response to vitamin D_3 treatment is the consequence of the significantly lower baseline levels because FGF23 levels were not significantly different in response to vitamin D_3 treatment between genotypes.

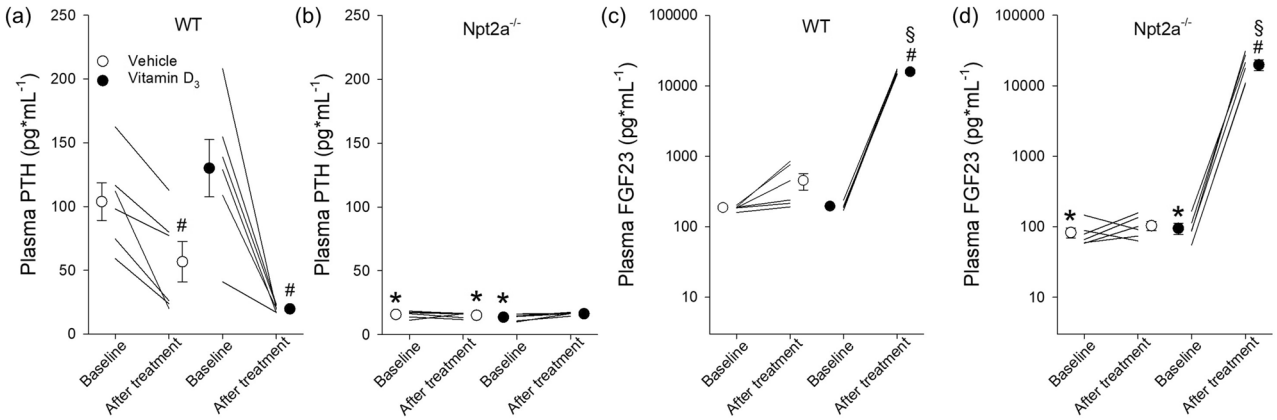

Figure 2. Vitamin D_3 induces divergent responses in plasma PTH and increases FGF23 in both WT or Npt2a$^{-/-}$ mice. Measurements of plasma PTH and FGF23 were performed in WT and Npt2a$^{-/-}$ mice following 4 days of treatment with either vehicle or vitamin D_3 (n = 6 per genotype). (**a**) In WT mice, vitamin D_3 treatment led to a decrease in plasma PTH levels. (**b**) In Npt2a$^{-/-}$ mice, plasma PTH levels were lower and unchanged in response to vitamin D_3 treatment. (**c** & **d**) FGF23 levels significantly increased in both genotypes in response to vitamin D_3 treatment. Male mice were used in these studies. In addition to single data summary data are shown and are expressed as mean ± SEM and were analyzed by repeated-measures two-way ANOVA followed by Tukey's multiple comparisons test. $^{*}P < 0.05$ vs WT same time point, $^{\#}P < 0.05$ vs baseline same genotype, $^{\S}P < 0.05$ vs vehicle same genotype and time point.

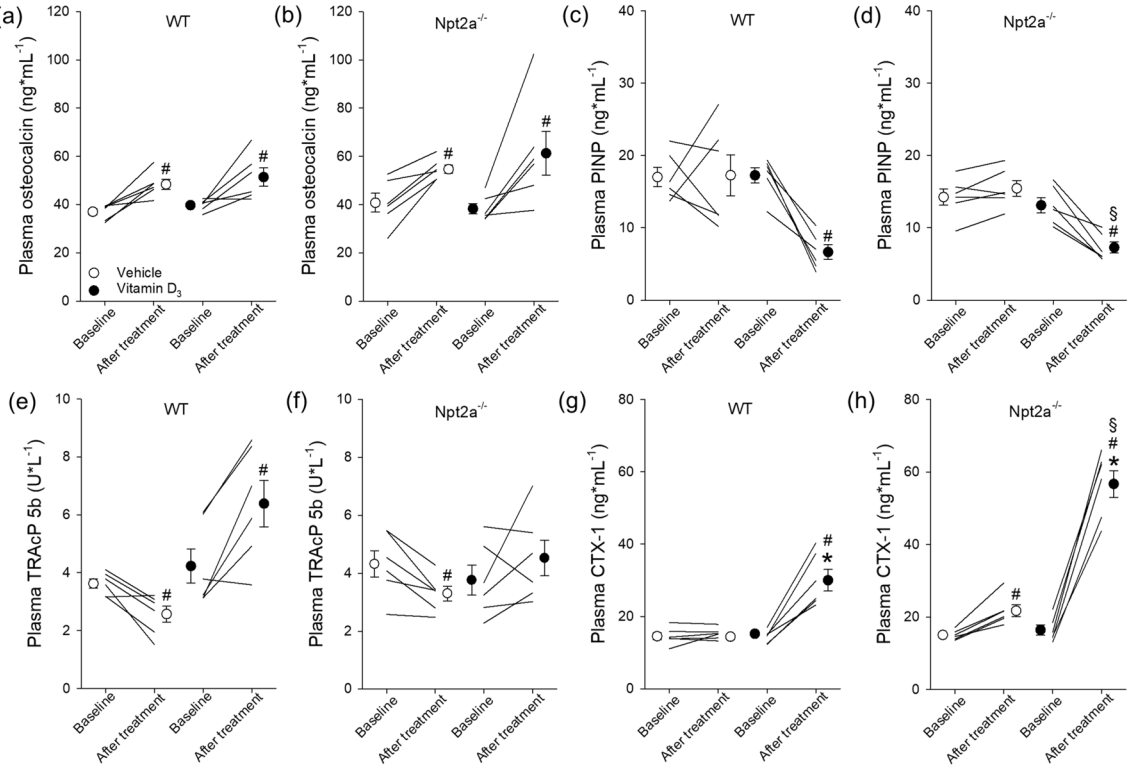

Figure 3. Npt2a determines the effects of Vitamin D_3 on bone remodeling markers. Circulating bone markers, including osteocalcin, PINP, TRAcP 5b, and CTX-1 were measured in WT and Npt2a$^{-/-}$ mice after 4 days of treatment with either a vehicle or vitamin D_3 (n = 6 per genotype). (**a** & **b**) Both genotypes show a small but significant increase in osteocalcin levels independent of treatment. (**c** & **d**) Vitamin D_3 decreased plasma PINP independent of genotype. (**e** & **f**) In both genotypes, vehicle treatment slightly but significantly decreased plasma TRAcP 5b levels but vitamin D_3 only significantly increased TRAcP 5b in WT mice. (**g** & **h**) Vitamin D_3 treatment increased CTX-1 levels in both genotypes but to a significantly greater extent in Npt2a$^{-/-}$ mice. Male mice were used in these studies. In addition to single data summary data are shown and are expressed as mean ± SEM and were analyzed by repeated-measures two-way ANOVA followed by Tukey's multiple comparisons test. $^{*}P < 0.05$ vs WT same time point, $^{\#}P < 0.05$ vs baseline same genotype, $^{\S}P < 0.05$ vs vehicle same genotype and time point.

Vitamin D_3 has distinct effects on bone remodeling markers in WT and Npt2a$^{-/-}$ mice

Since vitamin D_3 is instrumental for bone remodeling, we determined 2 bone formation markers (osteocalcin and PINP) and 2 bone resorption markers (TRAcP 5b and CTX-1) under baseline conditions and in response to vehicle or vitamin D_3 treatment. Under baseline conditions, no significant differences were observed in osteocalcin levels between genotypes, and vehicle and vitamin D_3 treatment resulted in a small but significant increase in osteocalcin levels independent of genotype (Fig. 3a,b). Plasma PINP levels were not significantly different between genotypes under baseline conditions, and vehicle treatment did not significantly change PINP levels in either genotype (Fig. 3c,d). Vitamin D_3 treatment significantly reduced (~ 60%) PINP levels in WT mice, and a similar reduction (~ 44%) was observed in Npt2a$^{-/-}$ mice. Plasma TRAcP 5b levels were not significantly different between genotypes under baseline conditions, and in both genotypes TRAcP 5b levels slightly but significantly decreased in response to vehicle treatment. Vitamin D_3 treatment significantly increased (~ 1.5-fold) TRAcP 5b levels in WT mice but was without significant effect in Npt2a$^{-/-}$ mice (Fig. 3e,f). Plasma CTX-1 levels were not significantly different between genotypes under baseline conditions, and vehicle treatment did not significantly affect CTX-1 levels in either genotype (Fig. 3g,h). Vitamin D_3 treatment significantly increased (~ twofold) CTX-1 levels in WT mice and even further increased (~ 3.5-fold) CTX-1 in Npt2a$^{-/-}$ mice. Consequently, CTX-1 levels were significantly higher in Npt2a$^{-/-}$ compared to WT mice after vitamin D_3 treatment (Fig. 3g,h).

Acute oral P_i loading results in greater plasma P_i levels in response to vitamin D_3 treatment compared to vehicle

In vehicle-treated WT and Npt2a$^{-/-}$ mice, acute oral P_i loading resulted in a significant increase in plasma P_i levels (2.4 ± 0.1 and 3.1 ± 0.1 mmol L^{-1}, respectively). In vitamin D_3-treated WT and Npt2a$^{-/-}$ mice, acute oral P_i loading resulted in a significantly greater increase in plasma P_i levels (3.9 ± 0.2 and 4.2 ± 0.3 mmol L^{-1}, respectively) compared to their respective vehicle-treated genotype (Fig. 4).

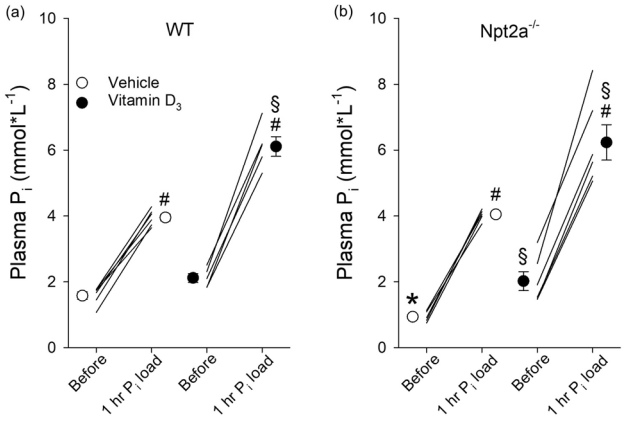

Figure 4. Similar effects of acute oral P_i loading on plasma P_i levels between genotypes. Plasma P_i levels were measured in WT and Npt2a$^{-/-}$ mice before and one hour after oral P_i loading via gavage (0.5 mol*L^{-1}, 1% of body weight). These measurements were performed following 4 days of treatment with either a vehicle or vitamin D_3 (n = 6 per genotype). (**a** & **b**) Oral P_i loading significantly increased plasma P_i levels independent of genotype or treatment; however, in vitamin D_3-treated mice the increase was significantly greater compared to vehicle-treated mice. Male mice were used in these studies. In addition to single data summary data are shown and are expressed as mean ± SEM and were analyzed by repeated-measures two-way ANOVA followed by Tukey's multiple comparisons test. *$P < 0.05$ vs WT same time point, $^{\#}P < 0.05$ vs baseline same genotype, $^{\S}P < 0.05$ vs vehicle same genotype and time point.

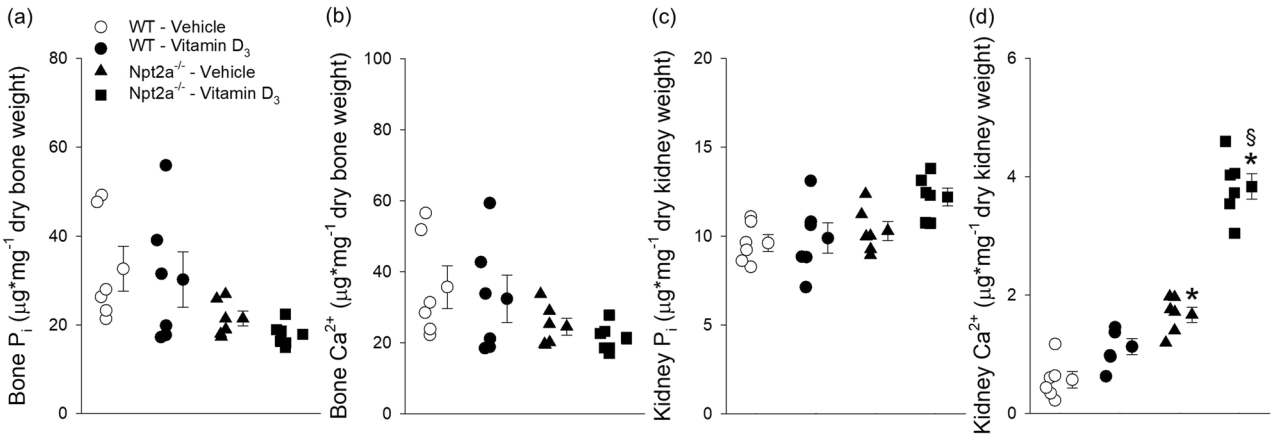

Figure 5. Vitamin D_3 treatment increases kidney Ca^{2+} levels in Npt2a$^{-/-}$ mice. Measurements of P_i and Ca^{2+} levels were carried out in bone and kidney tissues of WT and Npt2a$^{-/-}$ mice following 4 days of treatment with either a vehicle or vitamin D_3 (n = 6 per genotype). (**a** & **b**) There was no difference in the levels of P_i and Ca^{2+} in bone of either genotype in response to vehicle or vitamin D_3 treatment. (**c**) Kidney P_i levels were not significantly different between genotypes or treatment. (**d**) The kidney Ca^{2+} levels were significantly greater in response to vehicle treatment in Npt2a$^{-/-}$ compared to WT mice. Vitamin D_3 treatment was not associated with altered kidney Ca^{2+} levels in WT mice; however, resulted in the highest kidney Ca^{2+} levels in Npt2a$^{-/-}$ mice. Male mice were used in these studies. In addition to single data summary data are shown and are expressed as mean ± SEM and were analyzed by two-way ANOVA followed by Tukey's multiple comparisons test. *$P < 0.05$ vs WT same treatment, $^{\S}P < 0.05$ vs vehicle same genotype.

Vitamin D_3 treatment causes significant Ca^{2+} accumulation in the kidney of Npt2a$^{-/-}$ mice

Determination of Ca^{2+} and P_i amounts were conducted on ashed tissue from vehicle and vitamin D_3-treated WT and Npt2a$^{-/-}$ mice. Amounts of P_i or Ca^{2+} in bone were not significantly different between genotypes in response to vehicle or vitamin D_3 treatment (Fig. 5A,B). Similarly, kidney P_i levels were not significantly different between genotypes in response to vehicle or vitamin D_3 treatment (Fig. 5c). Of note, kidney Ca^{2+} levels in response to vehicle treatment were significantly greater (~ threefold) in Npt2a$^{-/-}$ compared to WT mice (Fig. 5d). Kidney Ca^{2+} levels were not significantly different between vehicle- and vitamin D_3-treated WT mice. In contrast, vitamin D_3 treatment in Npt2a$^{-/-}$ mice resulted in the highest kidney Ca^{2+} content observed between groups and genotypes and was ~ 3.5-fold greater compared to vitamin D_3-treated WT mice.

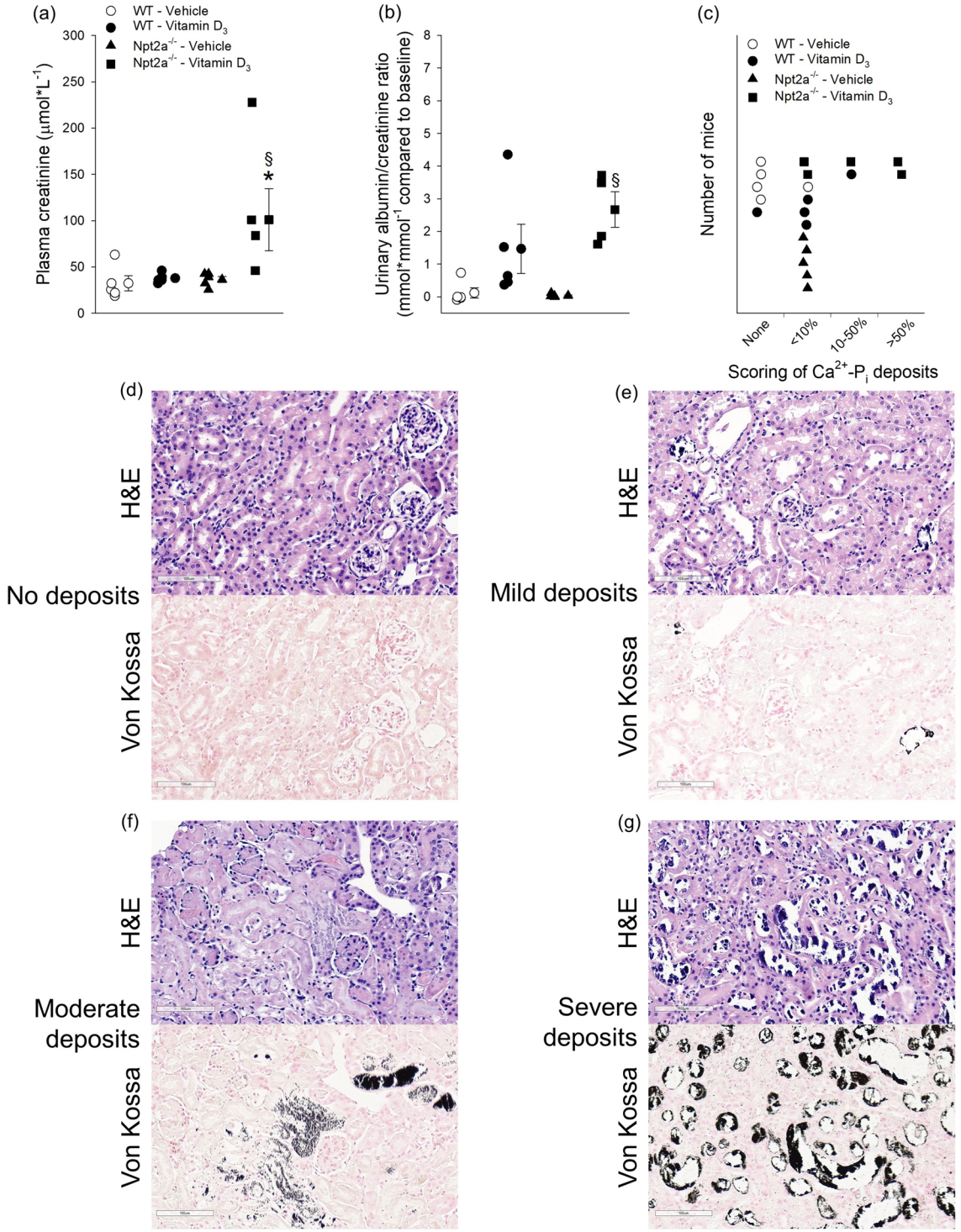

Figure 6. Vitamin D_3-treated Npt2a$^{-/-}$ mice show signs of impaired kidney function and greater renal Ca^{2+}-P_i deposits. (**a**) Plasma creatinine levels were the highest in vitamin D_3-treated Npt2a$^{-/-}$ mice. (**b**) Similarly, urinary albumin/creatinine ratios showed the biggest increase compared to baseline in vitamin D_3-treated Npt2a$^{-/-}$ mice. (**c**) Histological classification of mineral deposits in genotypes with vehicle or vitamin D_3 treatment. The majority of vehicle-treated WT mice show no mineral deposits, vehicle-treated Npt2a$^{-/-}$ mice showed mild deposits (< 10%), vitamin D_3-treated WT showed greater severity (moderate 10–50%) and only some vitamin D_3-treated Npt2a$^{-/-}$ mice showed the greatest number of deposits (> 50%). Representative examples of H&E and von Kossa staining are shown for each condition from mice with no mineral deposits (**d**), mild deposits (**e**), moderate deposits (**f**) and severe deposits (**g**). Von Kossa staining shows that Ca^{2+}-P_i crystal deposits (black stains) localize within the tubular lumen. The tubules show evidence of damage with attenuation of the epithelial lining. Magnification × 200. Scale bar of 100 µm is shown in each image. Male and female mice were used in these studies. In addition to single data summary data are shown and are expressed as mean ± SEM and were analyzed by two-way ANOVA followed by the two-stage linear step-up procedure of Benjamini, Krieger, and Yekutieli. *$P < 0.05$ vs WT same treatment, $^{§}P < 0.05$ vs vehicle same genotype.

Vitamin D_3 treatment causes signs of impaired renal function associated with severe renal Ca^{2+}-P_i deposits in Npt2a$^{-/-}$ mice

Plasma creatinine shows the highest levels in vitamin D_3-treated Npt2a$^{-/-}$ mice, no differences were observed between the other groups (Fig. 6a). Urinary albumin/creatinine ratios also showed significantly increased levels in vitamin D_3-treated Npt2a$^{-/-}$ mice compared to vehicle-treated Npt2a$^{-/-}$ mice (Fig. 6b). To visualize Ca^{2+}-P_i deposits, we used von Kossa staining and performed semi-quantitative analysis (Fig. 6c–g). Consistent with plasma creatinine levels, vitamin D_3-treated Npt2a$^{-/-}$ mice show the most severe amount (> 50%) of crystal deposits in the tubular lumen. The tubules show evidence of damage with attenuation of the epithelial lining. In contrast to vitamin D_3-treated Npt2a$^{-/-}$ mice, the majority of vitamin D_3-treated WT mice show only mild (< 10%) crystal deposits similar to vehicle-treated Npt2a$^{-/-}$ mice.

Renal mRNA expression

RT-qPCR profiling of genes (all shown in Supplementary Fig. 2) expressed in the kidney confirmed that primers for *Slc34a1* (Npt2a) were specific for Npt2a since no mRNA amplification was found in Npt2a$^{-/-}$ mice. Vehicle treatment showed significantly lower *CaSR* (Ca^{2+}-sensing receptor) and *Cldn19* (claudin-19) expression in Npt2a$^{-/-}$ compared with WT mice. In vitamin D_3-treated WT mice, significant differences in mRNA expression were found compared to vehicle treatment for *Slc34a1*, *Slc34a3* (Npt2c), *Slc8a1* (Na^+/Ca^{2+} exchanger, NCX1), *Atp2b4* (ATPase plasma membrane Ca^{2+} transporting 4), and *CaSR*. In vitamin D_3-treated Npt2a$^{-/-}$ mice, significant differences in mRNA expression were observed compared to vehicle treatment for *Slc34a3*, *Atp2b4*, *Trpv5* (transient receptor potential cation channel subfamily V member 5), *CaSR*, *Cyp27b1* (25-hydroxyvitamin D-1α-hydroxylase) and *Cldn16* (claudin-16). Significant differences between genotypes in response to vitamin D_3 treatment were found for *CaSR*, *Cyp27b1*, and *Cldn16*.

Npt2a maintains Npt2c and claudin-3 expression in response to vitamin D_3

Confirming the specificity of the Npt2a antibody, no Npt2a band was observed in kidney tissue of Npt2a$^{-/-}$ mice (Fig. 7a). In response to vitamin D_3 treatment in WT mice, Npt2a abundance was significantly lower (~65%) compared to vehicle-treated mice (Fig. 7a). Consistent with a compensatory response of Npt2c abundance in Npt2a$^{-/-}$ mice, Npt2c abundance was ~3.5-fold greater in vehicle-treated Npt2a$^{-/-}$ mice compared to vehicle-treated WT mice (Fig. 7b). In response to vitamin D_3 treatment in WT mice, Npt2c abundance was significantly

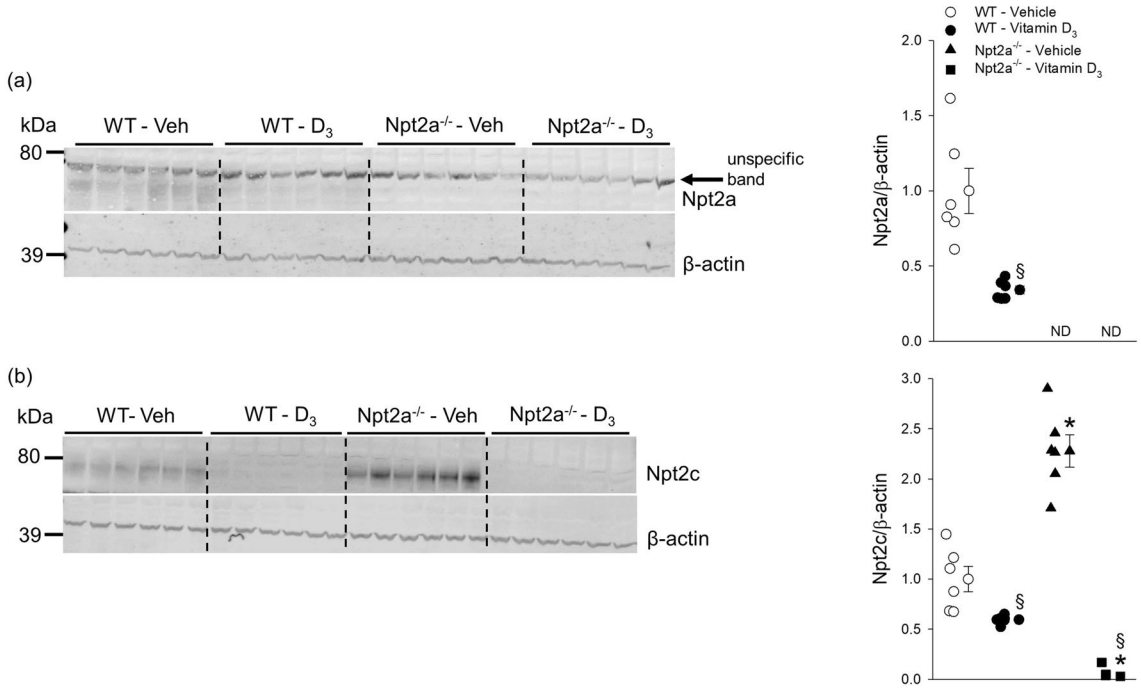

Figure 7. Npt2c abundance is diminished in Npt2a$^{-/-}$ mice in response to vitamin D_3 treatment. Abundance of Npt2a and Npt2c in kidney tissues of WT and Npt2a$^{-/-}$ mice after 4 days of treatment with vehicle or vitamin D_3 (n = 4–6 per genotype). (**a**) In this study we confirmed the specificity of the Npt2a antibody in Npt2a$^{-/-}$ mice, which lack the ~75–80 kDa band representing Npt2a. An unspecific band was detected. In WT mice, vitamin D_3 treatment showed lower Npt2a expression compared to vehicle treatment. (**b**) In response to vehicle treatment, Npt2c abundance was significantly greater in Npt2a$^{-/-}$ compared to WT mice. Npt2c abundance was significantly lower in vitamin D_3-treated mice; however, the level in Npt2a$^{-/-}$ mice was almost undetectable. Male mice were used in these studies. In addition to single data summary data are shown and are expressed as mean ± SEM and were analyzed by two-way ANOVA followed by Tukey's multiple comparisons test. *$P < 0.05$ vs WT same treatment, §$P < 0.05$ vs vehicle same genotype.

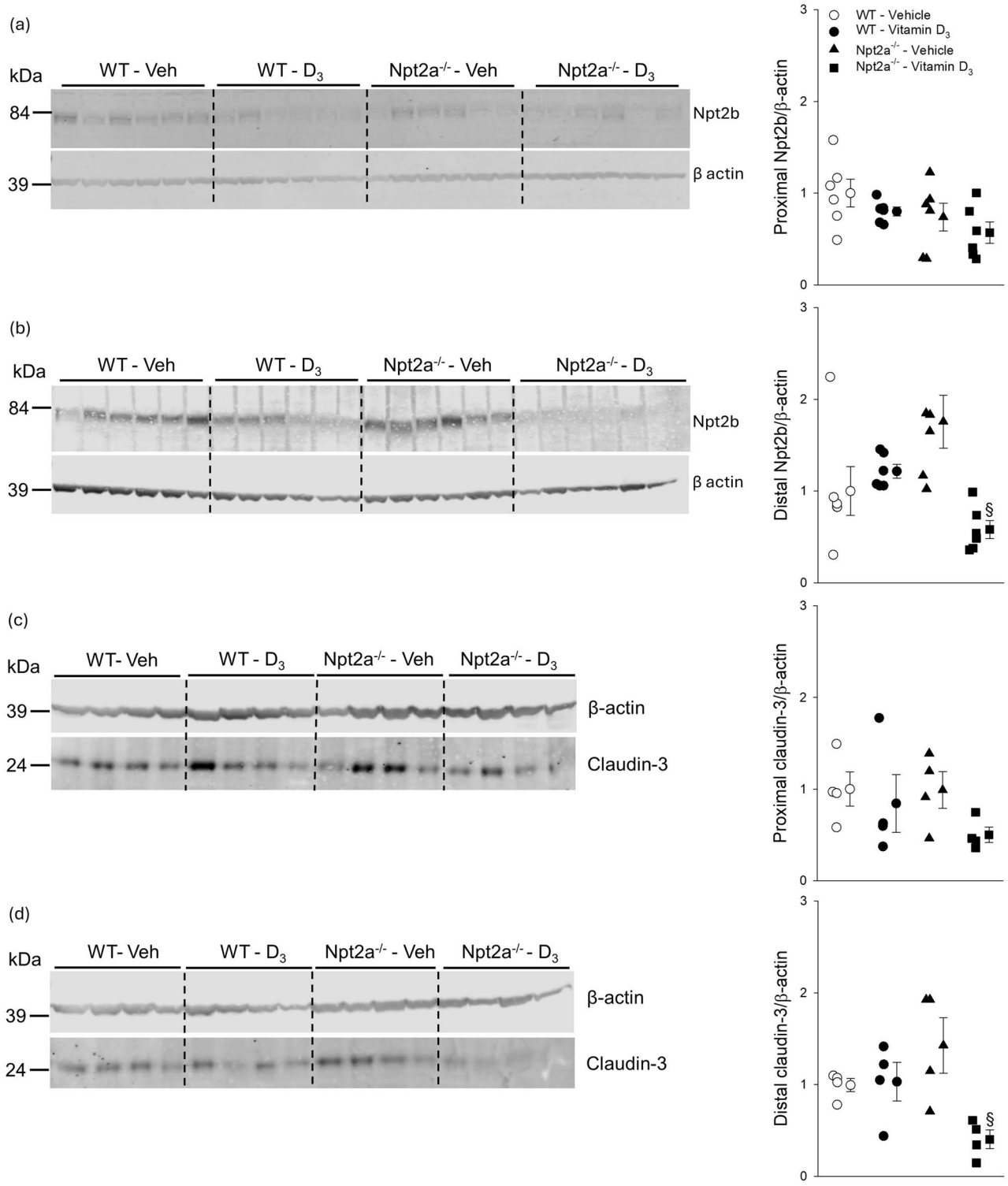

Figure 8. Npt2b abundance is diminished in Npt2a$^{-/-}$ mice in response to vitamin D_3 treatment. (**a**) Abundance of Npt2b in the proximal small intestine was not different between genotypes or treatment. (**b**) In the distal small intestine, no differences were detected in Npt2b abundance between vehicle-treated genotypes. In WT mice, Npt2b abundance was similar in response to vitamin D_3 compared to vehicle treatment. Of note, Npt2b abundance in vitamin D_3 -treated Npt2a$^{-/-}$ mice was lower compared to vehicle treatment. (**c**) Abundance of claudin-3 was somewhat variable in the proximal small intestine and no differences were observed between genotype or treatment. (**d**) In the distal small intestine, no differences in claudin-3 abundance were detected between vehicle-treated genotypes. In WT mice, claudin-3 abundance was similar in response to vitamin D_3 compared to vehicle treatment. Of note, claudin-3 abundance in vitamin D_3-treated Npt2a$^{-/-}$ mice was lower compared to vehicle treatment. Male mice were used in these studies. In addition to single data summary data are shown and are expressed as mean ± SEM and were analyzed by two-way ANOVA followed by Tukey's multiple comparisons test. $^{§}P < 0.05$ vs vehicle same genotype.

lower (~40%) compared to vehicle-treated WT mice. Of note, vitamin D_3 treatment completely diminished Npt2c abundance in Npt2a$^{-/-}$ mice. Since vitamin D_3 affects intestinal P_i transport, we further analyzed intestinal abundance of Npt2b and claudin-3, the latter being a paracellular tight junction protein involved in P_i transport[21]. The majority of intestinal P_i uptake in the mouse occurs in the distal small intestine[22,23]. The abundance of Npt2b in the proximal small intestine was not significantly different between genotypes or treatments (Fig. 8a). No differences were observed in the abundance of Npt2b in the distal small intestine between genotypes in response to vehicle treatment. In WT mice (Fig. 8b), Npt2b abundance was not significantly different in response to vitamin D_3 compared to vehicle treatment. In contrast, Npt2b expression in the distal small intestine of Npt2a$^{-/-}$ mice was significantly lower (~77%) in response to vitamin D_3 compared to vehicle treatment (Fig. 8b).

In the proximal small intestine of WT mice, claudin-3 protein abundance was not significantly different between vehicle or treatment groups (Fig. 8c). In the distal small intestine, no significant differences were observed in claudin-3 abundance between genotypes in response to vehicle treatment (Fig. 8d) and in WT mice no significant differences were observed between vehicle and vitamin D_3 treatment. In contrast, in Npt2a$^{-/-}$ mice, claudin-3 protein abundance was significantly lower (~72%) in response to vitamin D_3 compared to vehicle treatment (Fig. 8d).

Discussion

The role of Npt2a in regulating renal P_i transport has been extensively studied. However, there are significant knowledge gaps when it comes to the complex hormonal regulation of this transporter, in particular the role of vitamin D_3. To gain further mechanistic insight, we studied P_i and Ca^{2+} homeostasis when the body is challenged by exogenous administration of a high dose of vitamin D_3 in the absence and presence of hypophosphatemia, the latter caused by lack of Npt2a. Surprisingly, despite lack of Npt2a which should have facilitated renal P_i excretion, these mice show signs of impaired P_i excretion, possibly a results of greater nephrocalcinosis and a reduction of kidney function, in response to vitamin D_3 administration (for a summary see Fig. 9).

Lack of Npt2a causes hypophosphatemia[16,18,20], a finding confirmed in the current study. A similar situation can be induced by administration of a Npt2a inhibitor[20,24,25]. In WT mice, the administration of vitamin D_3 did not affect plasma P_i levels; in contrast, Npt2a$^{-/-}$ mice had a very uniform increase in plasma P_i following administration of vitamin D_3. Regarding the former, other studies which administered vitamin D_3 at a dose of 400,000 (IU kg^{-1}) to C57Bl/6 mice did not report changes in plasma P_i levels[26]. It is conceivable that in WT mice, the increase in urinary P_i/creatinine ratio served to stabilize plasma P_i levels. Consistent with this, vitamin D_3 treatment resulted in lower Npt2a and Npt2c expression in WT mice.

Under baseline conditions, we did not find a clear P_i wasting phenotype in Npt2a$^{-/-}$ mice. This could be related to a substantial compensatory greater Npt2c expression (seen on the protein but not mRNA level) which might

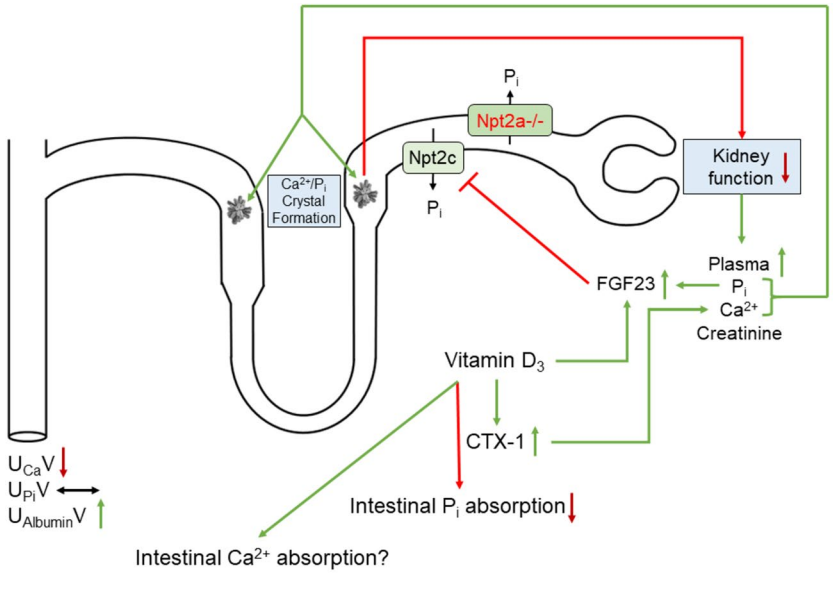

	WT VitD$_3$ vs. Veh	Npt2a$^{-/-}$ VitD$_3$ vs. Veh
Plasma P_i	⟷	↑
Plasma Ca^{2+}	↑	↑↑
Urinary P_i	↑	⟷
Urinary Ca^{2+}	↑	↓
Kidney function	⟷	↓
Renal calcification	Mild	Severe
Renal Npt2a	↓	Not detectable
Renal Npt2c	↓	Not detectable
Intestinal Npt2b	⟷	↓
Intestinal claudin-3	⟷	↓

Figure 9. Summary figure. In vitamin D_3-treated Npt2a$^{-/-}$ mice, a circulus vitiosus is observed leading to kidney failure. We hypothesize that vitamin D_3 treatment leads to elevated plasma Ca^{2+} levels (possibly via increased bone resorption as indicated by greater CTX-1 levels and/or increased intestinal Ca^{2+} absorption) and decreased intestinal P_i absorption (via lower Npt2b and claudin-3 levels). A combination of vitamin D_3, elevated plasma P_i, and reduced kidney function causes FGF23 levels to be drastically elevated, subsequently diminishing Npt2c abundance and leading to supersaturation of tubular fluid with Ca^{2+} and P_i. Formation of Ca^{2+}/P_i crystals lead to renal calcification and reduced kidney function (increase in plasma creatinine and urinary albumin). Consequently, plasma Ca^{2+} and P_i levels are further increased. Green arrows indicate an increase, red arrows indicate a decrease. The table on the right summarizes the most significant findings observed between vitamin D_3 treated mice and vehicle treated mice for both genotypes.

mitigate the P_i wasting phenotype. It is notable that plasma P_i significantly increased in response to vitamin D_3 treatment despite the absence of Npt2a. This corroborated with greater urinary albumin/creatinine ratios and greater plasma creatinine levels, possibly implying that reduced kidney function might have contributed to this finding. In addition, Npt2c abundance was also diminished in Npt2a$^{-/-}$ mice under these conditions, both of which should facilitate urinary P_i excretion and prevent a rise in plasma P_i. In terms of renal Npt2 transporter expression in response to vitamin D_3, Npt2a$^{-/-}$ mice resemble Npt2a/c double knockout mice. What could explain the lack of increase in urinary P_i/creatinine ratios in response to vitamin D_3 in Npt2a$^{-/-}$ mice? One possible explanation could be that urinary P_i excretion has reached a maximum. Consistent with this, we have previously shown in short-term metabolic cage experiments that urinary P_i/creatinine ratios in Npt2a$^{-/-}$ mice were of the same magnitude, and only acute Npt2a inhibition in control mice was able to double urinary P_i/creatinine[20], suggesting that in Npt2a$^{-/-}$ mice (chronically), despite the presence of compensatory mechanisms, no further increase in urinary P_i excretion can be achieved.

In terms of Ca^{2+}, our data are consistent with the previously published Npt2a$^{-/-}$ phenotype as well as the role of vitamin D_3 in Ca^{2+} homeostasis[16,18]. Npt2a$^{-/-}$ mice have higher plasma Ca^{2+} levels and greater urinary Ca^{2+}/creatinine ratios. Vitamin D_3 is a well-known regulator of intestinal Ca^{2+} absorption[27] and knockout of Npt2a is associated with significantly increased intestinal Ca^{2+} absorption, possibly as a consequence of greater intestinal mRNA expression of epithelial Ca^{2+} channels (ECaC1 and ECaC2) and the Ca^{2+} binding protein calbindin-D9k[28]. Vitamin D_3 treatment increased plasma Ca^{2+} in both genotypes, but to a greater amount in Npt2a$^{-/-}$ mice. Of note, one of the most interesting findings in this study relates to the response of the kidney after administration of vitamin D_3. In WT mice, urinary Ca^{2+}/creatinine was appropriately increased possibly as a consequence of significant hypercalcemia. In contrast to WT mice, in Npt2a$^{-/-}$ mice urinary Ca^{2+}/creatinine was reduced in response to vitamin D_3 administration, reaching levels seen in WT mice under baseline conditions. Consequently, the reduction of urinary Ca^{2+}/creatinine ratio could have contributed to the greater increase in plasma Ca^{2+} in Npt2a$^{-/-}$ mice. Despite vitamin D response elements being present in the CaSR gene causing up-regulation of CaSR expression[29], our study provides evidence that vitamin D_3 treatment can reduce CaSR expression.

Ultrastructural studies in Npt2a$^{-/-}$ mice showed that at early age Ca^{2+}/P_i deposits develop that were purged during later stages of life[30,31]. Along those lines, our tissue analysis showed that vitamin D_3-treated Npt2a$^{-/-}$ mice had the highest kidney Ca^{2+} content of all studied groups, without significant differences in kidney P_i content. Of note, Npt2a mutations in humans seem fairly common in a large cohort of Ca^{2+}-stone forming pedigrees, but they do not seem to corroborate with clinically significant P_i or Ca^{2+} handling abnormalities[32]. Our studies expand this knowledge and show that vitamin D_3-treated Npt2a$^{-/-}$ mice show the greatest amount of Ca^{2+}-P_i crystal deposits in the tubule lumen. Of note, vitamin D_3-treated WT mice show a similar pattern of Ca^{2+}-P_i crystal deposits compared to vehicle-treated Npt2a$^{-/-}$ mice. Taken together, Npt2a$^{-/-}$ mice have a significant problem in excreting Ca^{2+} in their urine and, considering also the lack of Npt2c in response to vitamin D_3 administration, their kidney Ca^{2+} content is further consistent with the phenotype of Npt2a/c double knockout mice, which show severe renal calcifications[18].

Possibly because of a combination of hypophosphatemia and hypercalcemia in Npt2a$^{-/-}$ mice, PTH and FGF23 levels are significantly lower compared to WT mice[16–18] which is still present when a high P_i or high P_i/Ca^{2+} diet is provided[17]. Under baseline conditions, these findings were confirmed in our study. PTH synthesis and release under these conditions seems to be under a dual control: (1) hypercalcemia inhibits the synthesis and secretion of PTH from the parathyroid gland via activation of the CaSR and (2) active vitamin D_3 suppresses the synthesis and release of PTH via activation of the VDR[33]. Of note, the changes observed cannot explain the paradoxical response of urinary Ca^{2+}/creatinine in Npt2a$^{-/-}$ mice in response to vitamin D_3. The situation in vitamin D_3-treated Npt2a$^{-/-}$ mice is similar to hereditary hypophosphatemic rickets with hypercalciuria[34] a physiology also resembled in Npt2a/c double knockout mice[18]. One notable difference is the accumulation of Ca^{2+} in the kidney of vitamin D_3-treated Npt2a$^{-/-}$ mice rather than the development of a hypercalciuric response. Along those lines, PTH was already substantially reduced in Npt2a$^{-/-}$ mice under baseline conditions possibly in the face of lower plasma P_i and elevated plasma Ca^{2+} levels. The decrease of PTH in WT mice in response to vehicle treatment possibly relates to the presence of ethanol which has been shown to decrease PTH levels[35,36].

Consistent with previous reports, our study confirms the lower FGF23 levels in Npt2a$^{-/-}$ mice, a possible consequence of lower plasma P_i levels[18]. Our study did not determine $1,25(OH)_2D_3$ levels but levels were found to be significantly greater in Npt2a$^{-/-}$ compared with WT mice[16,18]. Our data show that vitamin D_3 treatment does not affect *Cyp24a1* and *Cyp27b1* mRNA expression in WT mice. In chronic kidney disease, expression of *Cyp24a1* is increased possibly accounting for decreased $1,25(OH)_2D_3$ due to degradation[37]. Vehicle treatment in Npt2a$^{-/-}$ mice showed significantly lower expression compared to WT mice, possibly explaining the body's effort to increase $1,25(OH)_2D_3$ levels. Only in vitamin D_3-treated Npt2a$^{-/-}$ mice was *Cyp27b1* mRNA expression significantly increased, which is consistent with greater $1,25(OH)_2D_3$ production. Study participants treated with vitamin D_3 normally do not show increases in $1,25(OH)_2D_3$ levels[38], which is reflected in unchanged *Cyp27b1* levels in vitamin D_3-treated WT mice compared to vehicle treatment. However, in the absence of Npt2a this can be offset, and our data imply that *Cyp27b1* mRNA expression is paradoxically increased.

When VDR are knocked out in chondrocytes of mice, FGF23 expression in osteoblasts and consequently FGF23 plasma levels are significantly reduced, implying that VDR is a prerequisite in this signaling pathway[39]. Of note, exogenous administration of vitamin D_3 is a powerful stimulator of FGF23, leading to ~80–200-fold increase; however, the exact signaling pathway(s) causing this increase remain unclear and the relationship between these hormones is complex. Our results dispute the role of PTH being a major determining factor for FGF23 production (which was drastically suppressed in both genotypes), or suggest additional regulatory mechanisms, which has been demonstrated in vivo and in vitro as well as in mice with hyperparathyroidism[40,41]. Vice versa, our data are consistent with the notion that FGF23 reduces PTH synthesis directly[42].

Npt2a$^{-/-}$ mice show a skeletal phenotype characterized by delayed secondary ossifications at 21 days of age which are reversed at 45 days of age and are ultimately overcompensated at > 74 days of age[16], these effects are even more exaggerated in Npt2a/c double knockout mice[18]. Our study used highly sensitive bone remodeling markers as estimators, which, to our knowledge, have never been determined in Npt2a$^{-/-}$ mice. Despite significant differences in P_i and Ca^{2+} homeostasis between genotypes, our study did not identify changes in any of the bone remodeling markers studied under baseline conditions. This might relate to the fact that Npt2a$^{-/-}$ mice were of adult age when our studies were performed. Osteocalcin is predominantly produced and secreted by osteoblasts during bone formation[43]. Although low doses of vitamin D_3 can stimulate bone turnover, high doses can cause bone resorption[44]. Despite these results, our study did not provide any differences between treatment or genotype in terms of osteocalcin levels. A possible explanation could be the short-term experimental setup we employed. PINP is considered the most sensitive marker of bone formation[45], which has been reported to be under the control of PTH[46] and shows an inverse relationship with active vitamin D_3[47]. Consistent with this, both genotypes decreased PINP levels after vitamin D_3 administration, consistent with a role of reduced bone formation. Of note, this occurred despite a significant decrease of PTH in both genotypes.

TRAcP 5b is an osteoclast-derived marker of bone resorption.[48]. Our findings show that vitamin D_3 treatment increased TRAcP 5b in WT mice. So far, no correlations have been described between FGF23 and TRAcP 5b under normal conditions; however, in patients on evocalcet treatment (CaSR agonist) PTH, FGF23 and TRAcP 5b decreased over the 30 week treatment period[49]. Our data point toward a role of Npt2a in this process since Npt2a$^{-/-}$ mice lack a response in TRAcP 5b in response to vitamin D_3. CTX-1 is a marker for bone remodeling that is released when type 1 collagen is degraded[50]. The role of vitamin D_3 on CTX-1 is ambiguous, with several human studies showing no effect of vitamin D_3 supplementation on CTX-1 levels[51,52] whereas others show a positive correlation[47]. This might relate to the pre-existing conditions that were studied, e.g. presence or absence of vitamin D_3 deficiency. Of note, and consistent with our study, a study in humans showed a dose-dependent effect of vitamin D_3 bolus administration (up to 600,000 IU) on CTX-1 levels 1 day after administration[53]. This might explain an increase in fracture risk when elderly women are treated annually with a single high dose (500,000 IU) of vitamin D_3[54]. In addition, daily doses of 10,000 IU for 3 years also resulted in a significant increase of CTX-1 in healthy adults[44]. Lack of Npt2a possibly unravels that these mice are more susceptible for disturbed bone remodeling.

The intestine plays a vital role in P_i and Ca^{2+} absorption in order to regulate homeostasis in the body and vitamin D_3 has been implicated in this regulation[14,28]. Our acute P_i loading experiments confirm these findings: independent of genotype, the intestinal uptake of P_i was significantly greater in vitamin D_3-treated mice compared to vehicle-treated mice as evidenced by greater increases in plasma P_i levels in the face of reduced renal Npt2a/c abundance. Our studies on Npt2b abundance also expand the knowledge on spatial regulation, where abundance in response to Npt2b was unaffected in the proximal small intestine, which contrasts with the distal small intestine. Of note, the contribution of transcellular versus paracellular intestinal P_i transport is a highly debated topic[15,23], and claudin-3 has been implicated in the paracellular process. Supporting this hypothesis are data from claudin-3 knockout mice, which have enhanced intestinal P_i uptake[21]. Similar to Npt2b, no regulation of claudin-3 abundance in the proximal small intestine was found in our studies, but in the distal small intestine of Npt2a$^{-/-}$ mice, claudin-3 abundance was significantly reduced, possibly contributing to greater plasma P_i levels in Npt2a$^{-/-}$ mice. In the kidney we find evidence that claudin-16, expressed in the thick ascending limb and distal convoluted tubule, was significantly reduced in vitamin D_3-treated Npt2a$^{-/-}$ mice. Claudin-16 inactivating mutations in humans are associated with hypercalciuria and nephrocalcinosis[55,56], possibly suggesting that significantly reduced claudin-16 expression in our studies might have contributed to the phenotype of vitamin D_3-treated Npt2a$^{-/-}$ mice. Along those lines, claudin-16 interacts with Trpv5 since knockdown of claudin-16 delocalized Trpv5 from the luminal membrane[57]. In our study, Trpv5 was also significantly reduced in vitamin D_3-treated Npt2a$^{-/-}$ mice compared to vehicle-treated Npt2a$^{-/-}$ mice. Our data provide information on the regulation of Atp2b4, which was reduced in response to vitamin D_3 in both genotypes; however, knockout of Atp2b4 in mice did not cause a Ca^{2+} phenotype[58].

In summary, our data provide novel insight into the role of vitamin D_3 in the regulation of P_i and Ca^{2+} homeostasis in the context of Npt2a. One limitation of using mice to study P_i homeostasis relates to distinct differences in intestinal and renal P_i handling compared to humans. Despite the vitamin D_3 dose used in our studies is supraphysiological, significant differences were observed between genotypes that pinpoint to an important role of Npt2a (and possibly claudin-16) in renal calcification and consequently kidney function decline. It is noteworthy that vitamin D_3 treatment in Npt2a$^{-/-}$ mice resulted in a complete loss of Npt2c, and mice in terms of renal P_i transporter expression resembled Npt2a/c double knockout mice. Despite a complete lack of renal P_i transporters, Npt2a$^{-/-}$ mice experience greater plasma P_i levels, possibly a consequence of reduced intestinal claudin-3 abundance. Further, Npt2a$^{-/-}$ mice develop significantly greater plasma Ca^{2+} levels in response to vitamin D_3, possibly a consequence of impaired renal Ca^{2+} excretion with tissue accumulation of Ca^{2+}, implying that Npt2a can function as a switch between renal Ca^{2+} excretion and reabsorption. However, the contribution of Npt2c in this process cannot be excluded considering its absence in abundance in response to vitamin D_3 treatment in Npt2a$^{-/-}$ mice.

Methods

The animal experiments were conducted in compliance with the NIH Guide for Care and Use of Laboratory Animals, set by the National Institutes of Health (Bethesda, MD), received approval from the Institutional Animal Care and Use Committee (11201R) at the University of South Florida, and are reported in accordance with ARRIVE guidelines. Npt2a$^{-/-}$ mice were obtained from the Jackson Laboratory (strain# 004802, Bar Harbor, ME) and propagated by heterozygote breeding. Mice have been backcrossed to C57BL/6J for 9 generations. Only

male WT and Npt2a$^{-/-}$ mice, 3–5 months old, were used for the study. The specific pathogen free mice were group housed and kept in a controlled environment with a 12-h light–dark cycle (light off at 18:00) in isolated ventilated cages. They were provided with free access to standard rodent diet (TD.2018, containing 0.7% P_i and 1% Ca^{2+}, Envigo, Madison, WI) and drinking water. Genotype was determined by PCR amplification of genomic DNA, which was extracted from ear tissue samples. The genotyping was carried out in accordance with protocol # 29530 published on the Jackson Laboratory website.

Vitamin D_3 treatment

Wild-type and Npt2a$^{-/-}$ mice were randomized into two treatment groups: one vehicle (5% Ethanol, 5% Cremophor EL, and 90% water) or vitamin D_3 (3,000 and 300,000 IU/kg body weight, Alfa Aesar, Haverhill, MA) dissolved in vehicle[26]. Treatments were administered on 4 consecutive days via subcutaneous injections (2 μL g^{-1} body weight) by and investigator blinded to genotype and treatment. Blood samples were collected under brief isoflurane anesthesia from the retrobulbar plexus before and after the 4-day treatment period. Spontaneously voided urine was collected at the same time.

Analysis of plasma and urine samples

Clinical chemistry was performed utilizing commercially available assays, adapted for use with small sample volumes[20,23]. Concentrations of P_i and Ca^{2+} in both plasma and urine were measured using inorganic phosphorous reagent and calcium arsenazo III reagent respectively, (Pointe Scientific, Canton, MI)[59]. Urinary creatinine was measured by infinity creatinine liquid stable reagent (Thermo Fisher Scientific, Middletown, VA). Urinary albumin and plasma creatinine were determined as described previously[60,61]. PTH and intact FGF23 were measured according to the manufacturer instructions (Quidel, San Diego, CA). Markers for bone resorption (tartrate-resistant acid phosphatase isoform 5b [TRAcP 5b, Quidel] and type I collagen cross-linked C-telopeptide [CTX-1, Immunodiagnostic Systems]) and bone formation (procollagen type I N-propeptide [PINP, Immunodiagnostic Systems, Gaithersburg, MD] and osteocalcin [Quidel]) were measured using ELISAs.

Acute hyperphosphatemic model

Four days after the administration of either vehicle or vitamin D_3, WT and Npt2a$^{-/-}$ mice were subjected to gavage of 0.5 mol L^{-1} NaH_2PO_4, 1% of body weight by an investigator blinded to genotype[23,62]. Before gavage and 60 min after administration, blood samples were collected under brief isoflurane anesthesia. Plasma P_i was measured as described above.

Determination of Ca^{2+} and P_i content in the kidney

In another set of WT and Npt2a$^{-/-}$ mice, femurs and kidneys were harvested under terminal isoflurane anesthesia 4 days after the last administration of vehicle or vitamin D_3. The collected tissues were dried for 24 h at 50 °C. Following the drying process, the weight of each tissue was determined. Next, the tissues were incinerated at a temperature of 560 °C for 12 h in a muffle furnace (Thermolyne F48015-60, Thermo Fisher Scientific). The ashes from the incineration were dissolved in 0.75 mol L^{-1} HCl. Concentrations of Ca^{2+} and P_i in the dissolved samples were determined as described above.

Histological analysis of kidneys

In a separate cohort of mice kidneys were perfused in vivo through the left ventricle with 4% PFA in phosphate buffered saline under isoflurane anesthesia. After kidneys were removed, they were fixed overnight in the same solution and subsequently paraffin embedded and sectioned at 4–6 μm. After deparaffinization and rehydration, sections were stained with hematoxylin and eosin (H&E) and von Kossa (to determine mineral deposits). Sectioning and staining were performed by Reliance Pathology Partners, LLC (Tampa, FL). Quantification of Ca^{2+}-P_i deposits were performed using the following scheme: none, mild (< 10%), moderate (10–50%), or severe (> 50%). The highest score seen in sections was reported for each mouse. All scoring was performed by a pathologist (M.T.) blinded to sample identity.

Isolation of intestinal epithelial cells

Another cohort of mice was randomized to administration of either vehicle or vitamin D_3 as described above. Following the 4-day treatment, mice were anesthetized by isoflurane and their kidneys and small intestines removed. Isolation of intestinal epithelial cells (IEC) via Ca^{2+} chelation was performed as described previously[23,63,64]. The IEC pellets were prepared for immunoblotting as described below.

Western blotting

Collected IEC and kidneys were homogenized in a buffer composed of 250 mmol L^{-1} sucrose and 10 mmol L^{-1} triethanolamine (Sigma-Aldrich, St. Louis, MO) containing Halt protease inhibitor cocktail and Halt phosphatase inhibitor cocktail (both Thermo Fisher Scientific). The homogenate was then subjected to a centrifugation process at 1000×*g* for 15 min followed by generation of plasma membrane-enriched samples (by centrifugation of the supernatant at 17,000×*g*) for 30 min. The pellets that emerged from this process were then resuspended and prepared for Western blotting. Protein quantity was determined using a bicinchoninic acid assay (Thermo Fisher Scientific). Samples of equal concentration were made by the addition of Laemmli sample buffer (final concentration of 0.1 mol L^{-1} SDS and 15 mg L^{-1} DTT). Samples were heated at 65 ^{0}C for 15 min before immunoblotting. The samples were resolved on either NuPAGE 4–12% or 12% Bis–Tris gels in MOPS. Proteins were transferred to polyvinylidene difluoride membranes and immunoblotted with rabbit polyclonal antibodies against

Npt2a, Npt2b, Npt2c (each with a dilution of 1:1500, generous gift from M. Levi)[23,24,62], rabbit anti claudin-3 (dilution 1:1000, also rabbit-sourced, Thermo Fisher Scientific)[23], and mouse anti β-actin (dilution 1:30,000, Sigma-Aldrich). These targets were then detected with secondary antibodies designed for rabbit (IRDye® 800CW donkey anti-rabbit IgG, at a dilution of 1:5000) or mouse (IRDye® 680RD donkey anti-mouse IgG, also at a dilution of 1:5000), using an Odyssey® CLx detection system (LI-COR Biosciences, Lincoln, NE). Quantification of the band intensities was carried out using Image Studio Lite for densitometric analysis (LI-COR Biosciences).

Quantitative polymerase chain reaction from kidney and bone

Total RNA from kidney homogenates was extracted using Tri Reagent (Sigma-Aldrich) using a protocol adapted from the manufacturer's recommendations. Total RNA was quantified using a Synergy Neo2 plate reader (Agilent, Santa Clara, CA). One thousand ng RNA of kidney sample were used to produce cDNA using a Revert Aid First Strand cDNA Synthesis Kit (Thermo Fisher Scientific). Maxima SYBR Green/ROX qPCR Master Mix (Thermo Fisher Scientific) was used in conjunction with a QuantStudio 6 Pro (Applied Biosystems, Thermo Fisher Scientific) for amplification. Template concentration was 1 ng μl^{-1} cDNA per 10 µl reaction (performed in triplicate) and used in conjunction with primer pairs specific for *Slc8a1, Slc34a1, Slc34a3, Trpv5, Atp2b4, Cyp25a1, Cyp27b1, Cldn2, Cldn14, Cldn16, Cldn19,* and *CaSR* with actin used as a reference gene (all primer sequences are provided in the Supplementary Information). Data analysis used the $^{\Delta\Delta}$Ct method, i.e. cycle thresholds (Ct), were normalized to actin expression, and compared with control.

Statistical analyses

Data are expressed as mean ± S.E.M. Two-way ANOVA or repeated-measures two-way ANOVA followed by Tukey's multiple comparison tests, or two-way mixed-effects ANOVA followed by the two-stage linear step-up procedure of Benjamini, Krieger, and Yekutieli, as indicated in the figure legends, were used to test for significant differences between genotype and/or treatment. All data were analyzed via GraphPad Prism (Version 10.1, Boston, MA) or SigmaPlot (Version 14, San Jose, CA, USA). Significance was considered at $P < 0.05$.

Data availability

The data that support the findings of this study are available from the authors upon reasonable request.

Received: 9 March 2024; Accepted: 16 July 2024
Published online: 23 July 2024

References

1. Dusso, A. S., Brown, A. J. & Slatopolsky, E. Vitamin D. *Am. J. Physiol. Renal Physiol. 289*, F8–28 (2005). https://doi.org/10.1152/ajprenal.00336.2004
2. Underland, L., Markowitz, M. & Gensure, R. Calcium and phosphate hormones: Vitamin D, parathyroid hormone, and fibroblast growth factor 23. *Pediatr. Rev.* **41**, 3–11. https://doi.org/10.1542/pir.2018-0065 (2020).
3. Christakos, S., Dhawan, P., Verstuyf, A., Verlinden, L. & Carmeliet, G. Vitamin D: metabolism, molecular mechanism of action, and pleiotropic effects. *Physiol. Rev.* **96**, 365–408. https://doi.org/10.1152/physrev.00014.2015 (2016).
4. Bergwitz, C. & Juppner, H. Regulation of phosphate homeostasis by PTH, vitamin D, and FGF23. *Annu. Rev. Med.* **61**, 91–104. https://doi.org/10.1146/annurev.med.051308.111339 (2010).
5. Thomas, L. *et al.* Acute adaption to oral or intravenous phosphate requires parathyroid hormone. *J. Am. Soc. Nephrol.* **28**, 903–914. https://doi.org/10.1681/ASN.2016010082 (2017).
6. Juppner, H. Phosphate and FGF-23. *Kidney Int. Suppl.* **79**, S24-27. https://doi.org/10.1038/ki.2011.27 (2011).
7. Quarles, L. D. Role of FGF23 in vitamin D and phosphate metabolism: Implications in chronic kidney disease. *Exp. Cell Res.* **318**, 1040–1048. https://doi.org/10.1016/j.yexcr.2012.02.027 (2012).
8. Demay, M. B., Kiernan, M. S., DeLuca, H. F. & Kronenberg, H. M. Sequences in the human parathyroid hormone gene that bind the 1,25-dihydroxyvitamin D3 receptor and mediate transcriptional repression in response to 1,25-dihydroxyvitamin D3. *Proc. Natl. Acad. Sci. USA* **89**, 8097–8101. https://doi.org/10.1073/pnas.89.17.8097 (1992).
9. Kolek, O. I. *et al.* 1alpha,25-Dihydroxyvitamin D3 upregulates FGF23 gene expression in bone: The final link in a renal-gastrointestinal-skeletal axis that controls phosphate transport. *Am. J. Physiol. Gastrointest. Liver Physiol.* **289**, G1036-1042. https://doi.org/10.1152/ajpgi.00243.2005 (2005).
10. Avioli, L. V., Lee, S. W., McDonald, J. E., Lund, J. & DeLuca, H. F. Metabolism of vitamin D3–3H in human subjects: Distribution in blood, bile, feces, and urine. *J. Clin. Invest.* **46**, 983–992. https://doi.org/10.1172/JCI105605 (1967).
11. Rosenstreich, S. J., Rich, C. & Volwiler, W. Deposition in and release of vitamin D3 from body fat: Evidence for a storage site in the rat. *J. Clin. Invest.* **50**, 679–687. https://doi.org/10.1172/JCI106538 (1971).
12. Haussler, M. R. *et al.* New understanding of the molecular mechanism of receptor-mediated genomic actions of the vitamin D hormone. *Bone* **17**, 33S-38S. https://doi.org/10.1016/8756-3282(95)00205-r (1995).
13. Song, Y., Kato, S. & Fleet, J. C. Vitamin D receptor (VDR) knockout mice reveal VDR-independent regulation of intestinal calcium absorption and ECaC2 and calbindin D9k mRNA. *J. Nutr.* **133**, 374–380. https://doi.org/10.1093/jn/133.2.374 (2003).
14. Kido, S., Kaneko, I., Tatsumi, S., Segawa, H. & Miyamoto, K. Vitamin D and type II sodium-dependent phosphate cotransporters. *Contrib. Nephrol.* **180**, 86–97. https://doi.org/10.1159/000346786 (2013).
15. Hernando, N. *et al.* 1,25(OH)(2) vitamin D(3) stimulates active phosphate transport but not paracellular phosphate absorption in mouse intestine. *J. Physiol.* **599**, 1131–1150. https://doi.org/10.1113/JP280345 (2021).
16. Beck, L. *et al.* Targeted inactivation of Npt2 in mice leads to severe renal phosphate wasting, hypercalciuria, and skeletal abnormalities. *Proc. Natl. Acad. Sci. USA* **95**, 5372–5377. https://doi.org/10.1073/pnas.95.9.5372 (1998).
17. Li, Y. *et al.* Response of Npt2a knockout mice to dietary calcium and phosphorus. *PLoS One* **12**, e0176232. https://doi.org/10.1371/journal.pone.0176232 (2017).
18. Segawa, H. *et al.* Npt2a and Npt2c in mice play distinct and synergistic roles in inorganic phosphate metabolism and skeletal development. *Am. J. Physiol. Renal. Physiol.* **297**, F671-678. https://doi.org/10.1152/ajprenal.00156.2009 (2009).
19. Miedlich, S. U., Zhu, E. D., Sabbagh, Y. & Demay, M. B. The receptor-dependent actions of 1,25-dihydroxyvitamin D are required for normal growth plate maturation in NPt2a knockout mice. *Endocrinology* **151**, 4607–4612. https://doi.org/10.1210/en.2010-0354 (2010).

20. Thomas, L. *et al.* PF-06869206 is a selective inhibitor of renal P(i) transport: Evidence from in vitro and in vivo studies. *Am. J. Physiol. Renal. Physiol.* **319**, F541–F551. https://doi.org/10.1152/ajprenal.00146.2020 (2020).
21. Hashimoto, N. *et al.* Lithocholic acid increases intestinal phosphate and calcium absorption in a vitamin D receptor dependent but transcellular pathway independent manner. *Kidney Int.* **97**, 1164–1180. https://doi.org/10.1016/j.kint.2020.01.032 (2020).
22. Radanovic, T., Wagner, C. A., Murer, H. & Biber, J. Regulation of intestinal phosphate transport. I. Segmental expression and adaptation to low-P(i) diet of the type IIb Na(+)-P(i) cotransporter in mouse small intestine. *Am. J. Physiol. Gastrointest. Liver Physiol.* **288**, G496-500. https://doi.org/10.1152/ajpgi.00167.2004 (2005).
23. Xue, J. *et al.* Enhanced phosphate absorption in intestinal epithelial cell-specific NHE3 knockout mice. *Acta Physiol. (Oxf.)* **234**, e13756. https://doi.org/10.1111/apha.13756 (2022).
24. Thomas, L. *et al.* Pharmacological Npt2a inhibition causes phosphaturia and reduces plasma phosphate in mice with normal and reduced kidney function. *J. Am. Soc. Nephrol.* **30**, 2128–2139. https://doi.org/10.1681/ASN.2018121250 (2019).
25. Clerin, V. *et al.* Selective pharmacological inhibition of the sodium-dependent phosphate cotransporter NPT2a promotes phosphate excretion. *J. Clin. Invest.* **130**, 6510–6522. https://doi.org/10.1172/JCI135665 (2020).
26. Luong, T. T. D. *et al.* Acid sphingomyelinase promotes SGK1-dependent vascular calcification. *Clin. Sci. (Lond.)* **135**, 515–534. https://doi.org/10.1042/CS20201122 (2021).
27. Christakos, S. Vitamin D: A critical regulator of intestinal physiology. *JBMR Plus* **5**, e10554. https://doi.org/10.1002/jbm4.10554 (2021).
28. Tenenhouse, H. S. *et al.* Na/P(i) cotransporter (Npt2) gene disruption increases duodenal calcium absorption and expression of epithelial calcium channels 1 and 2. *Pflugers Arch* **444**, 670–676. https://doi.org/10.1007/s00424-002-0865-2 (2002).
29. Canaff, L. & Hendy, G. N. Human calcium-sensing receptor gene. Vitamin D response elements in promoters P1 and P2 confer transcriptional responsiveness to 1,25-dihydroxyvitamin D. *J. Biol. Chem.* **277**, 30337–30350. https://doi.org/10.1074/jbc.M201804200 (2002).
30. Khan, S. R. & Canales, B. K. Ultrastructural investigation of crystal deposits in Npt2a knockout mice: Are they similar to human Randall's plaques?. *J. Urol.* **186**, 1107–1113. https://doi.org/10.1016/j.juro.2011.04.109 (2011).
31. Chau, H., El-Maadawy, S., McKee, M. D. & Tenenhouse, H. S. Renal calcification in mice homozygous for the disrupted type IIa Na/Pi cotransporter gene Npt2. *J. Bone Miner. Res.* **18**, 644–657. https://doi.org/10.1359/jbmr.2003.18.4.644 (2003).
32. Lapointe, J. Y. *et al.* NPT2a gene variation in calcium nephrolithiasis with renal phosphate leak. *Kidney Int.* **69**, 2261–2267. https://doi.org/10.1038/sj.ki.5000437 (2006).
33. Ritter, C. S. & Brown, A. J. Direct suppression of Pth gene expression by the vitamin D prohormones doxercalciferol and calcidiol requires the vitamin D receptor. *J. Mol. Endocrinol.* **46**, 63–66. https://doi.org/10.1677/JME-10-0128 (2011).
34. Bergwitz, C. & Miyamoto, K. I. Hereditary hypophosphatemic rickets with hypercalciuria: Pathophysiology, clinical presentation, diagnosis and therapy. *Pflugers Arch* **471**, 149–163. https://doi.org/10.1007/s00424-018-2184-2 (2019).
35. Diez, A. *et al.* Acute effects of ethanol on mineral metabolism and trabecular bone in Sprague-Dawley rats. *Calcif. Tissue Int.* **61**, 168–171. https://doi.org/10.1007/s002239900317 (1997).
36. Laitinen, K., Tahtela, R. & Valimaki, M. The dose-dependency of alcohol-induced hypoparathyroidism, hypercalciuria, and hypermagnesuria. *Bone Miner* **19**, 75–83. https://doi.org/10.1016/0169-6009(92)90845-5 (1992).
37. Jones, G., Prosser, D. E. & Kaufmann, M. 25-Hydroxyvitamin D-24-hydroxylase (CYP24A1): Its important role in the degradation of vitamin D. *Arch Biochem. Biophys.* **523**, 9–18. https://doi.org/10.1016/j.abb.2011.11.003 (2012).
38. Turner, M. E. *et al.* The metabolism of 1,25(OH)(2)D(3) in clinical and experimental kidney disease. *Sci. Rep.* **12**, 10925. https://doi.org/10.1038/s41598-022-15033-9 (2022).
39. Masuyama, R. *et al.* Vitamin D receptor in chondrocytes promotes osteoclastogenesis and regulates FGF23 production in osteoblasts. *J. Clin. Invest.* **116**, 3150–3159. https://doi.org/10.1172/JCI29463 (2006).
40. Rhee, Y. *et al.* Parathyroid hormone receptor signaling in osteocytes increases the expression of fibroblast growth factor-23 in vitro and in vivo. *Bone* **49**, 636–643. https://doi.org/10.1016/j.bone.2011.06.025 (2011).
41. Kawata, T. *et al.* Parathyroid hormone regulates fibroblast growth factor-23 in a mouse model of primary hyperparathyroidism. *J. Am. Soc. Nephrol.* **18**, 2683–2688. https://doi.org/10.1681/ASN.2006070783 (2007).
42. Ben-Dov, I. Z. *et al.* The parathyroid is a target organ for FGF23 in rats. *J. Clin. Invest.* **117**, 4003–4008. https://doi.org/10.1172/JCI32409 (2007).
43. Manolagas, S. C. Osteocalcin promotes bone mineralization but is not a hormone. *PLoS Genet.* **16**, e1008714. https://doi.org/10.1371/journal.pgen.1008714 (2020).
44. Burt, L. A. *et al.* Effect of high-dose vitamin D supplementation on volumetric bone density and bone strength: A randomized clinical trial. *JAMA* **322**, 736–745. https://doi.org/10.1001/jama.2019.11889 (2019).
45. Gillett, M. J., Vasikaran, S. D. & Inderjeeth, C. A. (2021) The role of PINP in diagnosis and management of metabolic bone disease. *Clin. Biochem. Rev.* **42**, 3–10. https://doi.org/10.33176/AACB-20-0001
46. Bauer, D. C. *et al.* Short-term changes in bone turnover markers and bone mineral density response to parathyroid hormone in postmenopausal women with osteoporosis. *J. Clin. Endocrinol. Metab.* **91**, 1370–1375. https://doi.org/10.1210/jc.2005-1712 (2006).
47. Nair, S. *et al.* Effect of vitamin D levels on bone remodeling in healthy women. *Int. J. Endocrinol. Metab.* **18**, e100656. https://doi.org/10.5812/ijem.100656 (2020).
48. Halleen, J. M., Tiitinen, S. L., Ylipahkala, H., Fagerlund, K. M. & Vaananen, H. K. Tartrate-resistant acid phosphatase 5b (TRACP 5b) as a marker of bone resorption. *Clin. Lab* **52**, 499–509 (2006).
49. Shigematsu, T. *et al.* Evocalcet with vitamin D receptor activator treatment for secondary hyperparathyroidism. *PLoS One* **17**, e0262829. https://doi.org/10.1371/journal.pone.0262829 (2022).
50. Naylor, K. & Eastell, R. Bone turnover markers: Use in osteoporosis. *Nat. Rev. Rheumatol.* **8**, 379–389. https://doi.org/10.1038/nrrheum.2012.86 (2012).
51. Madar, A. A. *et al.* Effect of vitamin D(3)-supplementation on bone markers (serum P1NP and CTX): A randomized, double blinded, placebo controlled trial among healthy immigrants living in Norway. *Bone Rep.* **2**, 82–88. https://doi.org/10.1016/j.bonr.2015.05.004 (2015).
52. Jorde, R. *et al.* Effects of vitamin D supplementation on bone turnover markers and other bone-related substances in subjects with vitamin D deficiency. *Bone* **124**, 7–13. https://doi.org/10.1016/j.bone.2019.04.002 (2019).
53. Rossini, M. *et al.* Dose-dependent short-term effects of single high doses of oral vitamin D(3) on bone turnover markers. *Calcif. Tissue Int.* **91**, 365–369. https://doi.org/10.1007/s00223-012-9637-y (2012).
54. Sanders, K. M. *et al.* Annual high-dose oral vitamin D and falls and fractures in older women: A randomized controlled trial. *JAMA* **303**, 1815–1822. https://doi.org/10.1001/jama.2010.594 (2010).
55. Muller, D. *et al.* A novel claudin 16 mutation associated with childhood hypercalciuria abolishes binding to ZO-1 and results in lysosomal mistargeting. *Am. J. Hum. Genet.* **73**, 1293–1301. https://doi.org/10.1086/380418 (2003).
56. Weber, S. *et al.* Novel paracellin-1 mutations in 25 families with familial hypomagnesemia with hypercalciuria and nephrocalcinosis. *J. Am. Soc. Nephrol.* **12**, 1872–1881. https://doi.org/10.1681/ASN.V1291872 (2001).
57. Hou, J. *et al.* Phosphorylated claudin-16 interacts with Trpv5 and regulates transcellular calcium transport in the kidney. *Proc. Natl. Acad. Sci. USA* **116**, 19176–19186. https://doi.org/10.1073/pnas.1902042116 (2019).
58. van Loon, E. P. *et al.* Calcium extrusion pump PMCA4: A new player in renal calcium handling?. *PLoS One* **11**, e0153483. https://doi.org/10.1371/journal.pone.0153483 (2016).

59. Thomas, L., Xue, J., Dominguez Rieg, J. A. & Rieg, T. Contribution of NHE3 and dietary phosphate to lithium pharmacokinetics. *Eur. J. Pharm. Sci.* **128**, 1–7. https://doi.org/10.1016/j.ejps.2018.11.008 (2019).
60. Vallon, V. *et al.* SGLT2 inhibitor empagliflozin reduces renal growth and albuminuria in proportion to hyperglycemia and prevents glomerular hyperfiltration in diabetic Akita mice. *Am. J. Physiol. Renal Physiol.* **306**, F194-204. https://doi.org/10.1152/ajprenal.00520.2013 (2014).
61. Vallon, V. *et al.* A role for the organic anion transporter OAT3 in renal creatinine secretion in mice. *Am. J. Physiol. Renal Physiol.* **302**, F1293-1299. https://doi.org/10.1152/ajprenal.00013.2012 (2012).
62. Fenton, R. A. *et al.* Renal phosphate wasting in the absence of adenylyl cyclase 6. *J. Am. Soc. Nephrol.* **25**, 2822–2834. https://doi.org/10.1681/ASN.2013101102 (2014).
63. Fenton, R. A. *et al.* Adenylyl cyclase 6 expression is essential for cholera toxin-induced diarrhea. *J. Infect. Dis.* **220**, 1719–1728. https://doi.org/10.1093/infdis/jiz013 (2019).
64. Xue, J. *et al.* An inducible intestinal epithelial cell-specific NHE3 knockout mouse model mimicking congenital sodium diarrhea. *Clin. Sci. (Lond.)* **134**, 941–953. https://doi.org/10.1042/CS20200065 (2020).

Author contributions

L.T. and T.R. conceived and designed research; L.T., L.V.D, M.T., S.A.M. and T.R. performed experiments; L.T., L.V.D, M.T. and T.R. analyzed data; L.T., L.V.D, M.T., A.S., J.A.D.R. and T.R. interpreted results of experiments; L.T., M.T. and T.R. prepared figures; L.T. and T.R. drafted manuscript; L.T., L.V.D., M.T., A.S., S.A.M., J.A.D.R., and T.R. edited and revised manuscript; L.T., L.V.D., M.T., A.S., S.A.M., J.A.D.R., and T.R. approved final version of manuscript.

Funding

This work was supported by the National Institute of Diabetes and Digestive and Kidney Diseases 1R01DK110621 (to T.R.) and VA Merit Review Awards IBX004968A (to T.R.) and IBX004024 (to A.S.). Additional support was provided by a Pilot Project from the USF Microbiomes Institute (to T.R. and J.D.R). The contents do not represent the views of the U.S. Department of Veterans Affairs or the United States Government.

Competing interests

The authors declare no competing interests.

Additional information

Supplementary Information The online version contains supplementary material available at https://doi.org/10.1038/s41598-024-67839-4.

Correspondence and requests for materials should be addressed to T.R.

Reprints and permissions information is available at www.nature.com/reprints.

Publisher's note Springer Nature remains neutral with regard to jurisdictional claims in published maps and institutional affiliations.